



Utilizing waste heat gasoline engine in the design and fabrication of a fin and tube evaporator for the Organic Rankine Cycle (ORC)



Awaludin Martin*, Rudi Hartono, Reza Asrian

Department of Mechanical Engineering, Faculty of Engineering, Riau University, Indonesia

Abstract

The excessive consumption of fossil fuels is causing environmental problems, which can be addressed by utilizing renewable energy sources such as hydro energy, biomass, solar heat, geothermal, and waste heat. In particular, the exhaust gas from gasoline engines presents an opportunity for energy recovery, as only 25% of the energy is utilized while the remaining 75% is wasted. A fin and tube type evaporator was designed, manufactured, and tested to utilize this exhaust gas in an Organic Rankine Cycle (ORC) system. The evaporator was designed with an outer tube diameter of 9.525 mm and a total tube length of 41.4 m, featuring 90 tubes and 135 fins with a total area of 14,325 m². It achieved an average effectiveness of 94.33%. The results showed that the waste heat from the exhaust gas of a gasoline engine could be used as a source of energy in an ORC system with an efficiency of 2.13%. It results in 7.02 kJ/s of energy absorbed by the evaporator and a net power generated of 0.15 kJ/s. This research demonstrates the potential for utilizing waste heat from gasoline engines as an energy source to generate electricity.

This is an open access article under the [CC BY-SA](#) license



Keywords:

Evaporator;
Organic Rankine Cycle;
Waste Heat;

Article History:

Received: May 25, 2022
Revised: October 14, 2022
Accepted: October 23, 2022
Published: June 2, 2023

Corresponding Author:

Awaludin Martin
Department of Mechanical
Engineering, Faculty of
Engineering, Riau University,
Indonesia
Email:
awaludinmartin01@gmail.com

INTRODUCTION

Electricity demand is rising, driven by several factors, such as population growth, economic development, and technological progress [1][2]. In Indonesia, the population has increased from 238 million in 2010 to 268 million in 2019, which is expected to further increase the per capita demand for electricity [3]. Projections from the National Energy Council indicate that the demand for electricity per capita is expected to reach 2,030 kWh/capita in 2025 and 6,723 kWh/capita in 2050. These projections are still within the targets the National Energy Policy set, which aims for 2,500 kWh/capita in 2025 and 7,500 kWh/capita in 2050 [4].

Indonesia's national energy consumption for electricity generation in 2018 was primarily sourced from fossil fuels, with petroleum, coal, and natural gas accounting for 7.13%, 48.65%, and 29.15% of the total consumption, respectively, totalling 84.93% [5]. However, using these fuels

has led to various environmental problems, such as air pollution, ozone layer depletion, acid rain, and global warming. These problems seriously affect human health, leading to respiratory illnesses, inflammation, heart diseases, and cancer. Additionally, the consumption of fossil fuels is unsustainable due to their limited availability [6, 7, 8].

As global energy demand continues to rise, finding sustainable solutions that reduce reliance on fossil fuels is becoming increasingly important. One promising approach is to increase the utilization of renewable energy sources, such as hydropower, ocean power, wind energy, biomass, solar power, and waste management [9][10]. Recent years have seen significant research efforts directed towards converting low-temperature and high-pressure heat into usable energy. Waste heat recovery has emerged as a promising technology among these approaches. Waste heat can be derived from various thermal

processes and significantly reduce dependence on fossil fuels while meeting global electricity demands. Unfortunately, conventional power generation methods are not very efficient at converting the heat obtained from these sources into electricity [11, 12, 13].

Waste heat recovery has the potential to enhance the performance of fuel combustion engines greatly. This is due to factors such as the engine's design, combustion efficiency, and heat transfer losses, which make it challenging to convert combustion heat into useful power [14] efficiently. It is estimated that conventional fuel combustion engines lose around 5% of their energy to friction, which accounts for about 25% of the energy used by the engine's fuel. The remaining 70% of energy is wasted as heat, carried away by exhaust gases and engine cooling systems. Therefore, the recovery of waste heat is critical for reducing energy consumption and emissions [15].

The Organic Rankine Cycle (ORC) system is a highly versatile technology that offers a range of benefits when it comes to utilizing low-temperature and low-pressure heat sources. By allowing organic working fluids to be indirectly evaporated through a heat exchange process, the ORC system enables the transformation of otherwise wasted energy into useful output. This means that low-temperature heat sources, such as solar heat, biomass, waste heat from engines, exhaust gas from industry, and geothermal energy, can be harnessed highly efficiently, reducing thermal pollution and lowering fossil fuel consumption [16][17]. Furthermore, the ORC technology boasts a range of other advantages, including high efficiency, simple layout, excellent partial load performance, quick startup and shutdown, and full automation without the need for highly qualified operators to be present at the plant [18].

The proper design of the evaporator is crucial to ensure efficient waste heat recovery in combined ORC and diesel systems. The evaporator's primary function is to facilitate heat exchange between the engine exhaust and the organic working fluid, making it a critical component in the ORC system. The evaporator's design and construction can significantly impact the system's size and overall performance. Therefore, optimising the evaporator's design parameters, such as the number of tubes and fins, tube diameter, and length, is essential to achieve optimal heat transfer rates and maximum energy efficiency [19].

Many studies have been conducted on ORC system. For example, according to Anastasovski et al., integrating ORC systems with

wastewater treatment plants can significantly increase system efficiency and total power output. Their study found that such integration improved system efficiency by up to 2.3%, resulting in an increase in total power output. In fact, the ORC system generated around 8.6% of the total electricity generated based on their research [20].

Martin et al. studied the ORC system using R134a as the working fluid and two different heat sources, a water heater and a solar collector. The research findings showed that the ORC system using the water heater as the heat source produced a theoretical power output of 279.58 watts with an efficiency of 3.33%. On the other hand, the ORC system using the solar collector as the heat source had a higher theoretical power output of 305 watts with an efficiency of 4.30%. These results indicate that ORC systems have the potential to utilize various heat sources, including renewable energy sources like solar energy, to enhance energy efficiency [21][22].

Loni et al. conducted a study utilizing solar collectors as the heat source, and their research showed that a system efficiency of over 20% could be achieved with parabolic trough collectors (PTCs). The study concluded that PTCs are an effective option for ORC applications to achieve high efficiency at an affordable cost [23].

In a study by Ahmadi et al., geothermal energy was used as a heat source for an ORC system by using R134a and R245fa as working fluids. The results showed that the power output from 1 kg/s of R134a was 17.5 kW, while the power output increased to 22.5 kW when R245fa was used. The geothermal heat source temperature was maintained at around 70°C for both cases. Economic analysis of the study indicated that the cost of electricity generation using R134a and R245fa was \$0.17/kWh and \$0.14/kWh, respectively [24].

The performance of an ORC's performance largely depends on its heat exchanger's efficiency and stability. Numerous studies have been conducted to optimize heat exchanger design to improve performance. For example, Sudiono et al. increased the number of circular turbulators in a heat exchanger to enhance efficiency. Their study, which utilized a PVC outer tube and a copper alloy inner tube with fiberglass turbulators, found that incorporating seven circular turbulators improved heat transfer rate by 30% and reduced pressure drop by 80% compared to the section without circular turbulators, at a flow rate of 7 L/min of cool water [25].

Another study by Romahadi et al. optimized the design of a condenser to minimize pressure drop. They found that the CF-8.72(c) surface type, with a heat transfer area of 0.259 m², a total tube

length of 9.5 m, and a cross-tube length of 0.594 m, resulted in a pressure drop of 3778 Pa on the tube side, which meets most requirements. These studies highlight the important role that well-designed heat exchangers and condensers play in achieving optimal ORC system performance [26].

This study aims to design, manufacture, and test an ORC system utilizing a fin-and-tube type evaporator as a heat exchanger to capture waste heat from the exhaust of a gasoline engine.

METHOD

In this design research, a schematic and detailed description of an ORC system has been presented in Figure 1, which utilizes exhaust heat from a gasoline engine and a fin and tube type evaporator as a heat exchanger. The provided schematic demonstrates the functioning of the ORC system, including two cycles: the ORC cycle (green line) and the cooling cycle (blue line), with waste heat depicted by a red line. To ensure optimal performance of the ORC system, each component is equipped with a pressure gauge and a thermocouple to measure the pressure and temperature of the working fluid during operation.

It is worth noting that the exhaust from the gasoline engine is not used as a heat source for the ORC system but only as a means to provide a thermocouple reading for data collection and analysis. The actual heat source for the ORC system comes from the working fluid, which is circulated through a heat exchanger where it absorbs heat from a high-temperature source, such as geothermal or solar energy. The mass flow rate of the working fluid is typically measured using a flow meter, which enables accurate monitoring and control of the system's performance.

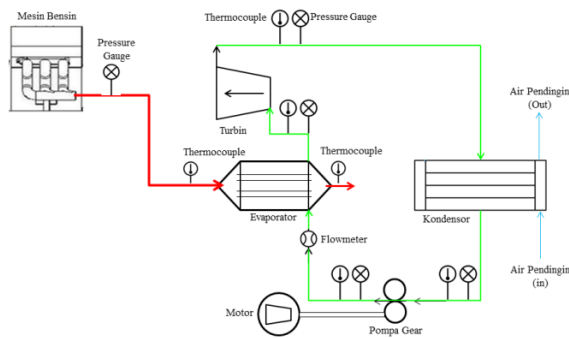


Figure 1. Schematic of ORC System

Evaporator Design

In this research, the evaporator arrangement was staggering, as shown in Figure 2. The design will be calculated using the following equations:

Total Effective Surface Area:

$$A_{Total} = A_{tube} + A_{fin} \tag{1}$$

The effective surface area is the coverage area of the tube, with the fluid flowing outside the tube [27].

$$A_{tube} = \pi \cdot d_o \cdot (L_2 - t_f \cdot N_f) \cdot N_{Tube} \tag{2}$$

The total area of the fin is:

$$A_{fin} = 2 \left(L_1 \cdot L_3 - \frac{\pi}{4} d^2 N_{tube} \right) N_{fin} + 2 L_3 \cdot t_{fin} \cdot N_{fin} \tag{3}$$

Frontal Area (Afr) is formulated with the following equation:

$$A_{fr, Udara} = L_2 \cdot L_3 \tag{4}$$

Minimum Free flow area (A#):

$$A_{ff} = \left\{ \left(\frac{L_3}{P_t} - 1 \right) z + [(S_T - d_r) - (S_T - d_o) \cdot t_f \cdot N_f] \right\} \tag{5}$$

Where Z is as follows:

$$Z = 2a \text{ if } 2a < 2b$$

$$Z = 2b \text{ if } 2b < 2a$$

Where: $2a = (X_T - d_r) - (X_L - d_r) \cdot t_f \cdot N_f$

$$b = \left[\left(\frac{X_T}{2} \right)^2 + (X_L)^2 \right]^{0,5} - d_r - (X_T - d_r) \cdot t_f \cdot N_f$$

Ratio of free flow to frontal area:

$$\sigma = \frac{L_2 \cdot L_3 - L_2 \cdot L_3 \cdot t_f \cdot N_f}{L_2 \cdot L_3} \text{ atau } \sigma = \frac{A_{ff}}{A_{Fr}} \tag{6}$$

Ratio of total heat transfer area to volume (α):

$$\alpha = \frac{A_{tot}}{V} \tag{7}$$

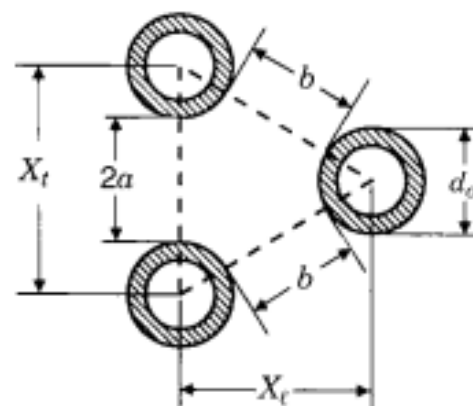


Figure 2. Unit cell of a staggered tube arrangement

Fin Efficiency

It can calculate the area of the fins to determine their efficiency and thus evaluate their performance. Fin efficiency is defined as the ratio between the heat transfer rate by the fins and the maximum heat transfer rate. In general, the fin's efficiency can be formulated as follows [27]:

$$\eta_f = \frac{\tanh(mL)}{mL} \quad (8)$$

From (8), the ratio of the actual heat delivered through one fin to its maximum condition, where the temperature of the fin is the same as the base temperature, can be calculated, thereby revealing the importance of fins in heat conduction. The above equation is used to determine the efficiency of a single fin. As the heat exchanger is made up of numerous fins, the efficiency used is the total surface efficiency, which is as follows [27]:

$$\eta_o = 1 - \frac{A_f}{A} (1 - \eta_f) \quad (9)$$

After calculating the surface geometry and fin efficiency, the heat transfer rate must be computed. To determine the values of Q_h and Q_c, the following equation is utilized [28]:

$$Q_h = Q_c = \dot{m} \cdot \Delta h \quad (10)$$

The method that is often used for the initial design of a heat exchanger is the LMTD (Log Mean Temperature Difference) method. The heat transfer rate equation with the LMTD method is as follows [28]:

$$q = U \cdot A \cdot \Delta T_{mean} \quad (11)$$

Where:

q = heat transfer rate (W)

U = Overall heat transfer coefficient (W/m²K)

A = Heat transfer surface area (m²)

ΔT_{LMTD} = Average temperature difference (K)

After that, the next step is to calculate the value of the Logarithmic Mean Temperature Difference (LMTD) or denoted by ΔT_{mean} [28]:

$$\Delta T_{mean} = LMTD = \frac{\Delta T_1 - \Delta T_2}{\ln \left(\frac{\Delta T_1}{\Delta T_2} \right)} \quad (12)$$

The next step is to calculate the value of the fluid flow velocity using the following equation [28]:

$$V = \frac{\dot{m}_h}{\rho \cdot A} \quad (13)$$

Where V, the velocity of the fluid, will be used to calculate the Reynolds number so that it can determine the type of flow of the fluid, the equation used is [28]:

$$Re = \frac{\rho V D}{\mu} \quad (14)$$

The Nusselt number is determined based on the type of fluid flow, laminar or turbulent, and the type of flow convection forces, whether internal or external. Usually, in fin and tube heat exchangers, internal forced convection is the fluid inside the tube, while external forced convection is outside the tube.

The Nusselt number equation for internal and external forced convection for laminar and turbulent flow is as follows [28]:

Internal forced:

Laminar

$$Nu = 3,66 + \frac{0,065 \left(\frac{D}{L} \right) Re Pr}{1 + 0,04 \left[\left(\frac{D}{L} \right) Re Pr \right]^{1/3}} \quad (15)$$

Turbulent

$$Nu = 0.023 \times Re^{0.8} Pr^{1/3} \quad (16)$$

External forced:

$$Nu = 0.35 \left(\frac{S_T}{S_L} \right)^{0.2} \times Re^{0.6} Pr^{0.36} \left(\frac{Pr}{Pr_s} \right)^{0.25} \quad (17)$$

After the Nusselt number is known, then calculate the heat transfer rate using equation [28]:

$$h = \frac{k}{D} Nu \quad (18)$$

To calculate the total value of thermal resistance (R) using the equation:

$$R_{total} = R_{conv,1} + R_{cond,fin} + R_{cond,tube} + R_{conv,2} \quad (19)$$

Next is to calculate the overall heat coefficient, U, by iterating so that the input U value is the same or almost the same as the output value or the final result. To calculate the value of U using an equation [28]:

$$U = \frac{1}{R} \quad (20)$$

The next step is to calculate the surface area (A) and the total length of the evaporator tube (L) using equation [28]:

$$A_{total} = \frac{Q}{U \cdot \Delta T_{lm}}$$

$$L_{total} = \frac{A_{tube}}{\pi D} \quad (21)$$

After that, the next calculation for the number of tubes (N_t) using the following equation:

$$A_{tube} = \pi D_o L N_T$$

$$N_T = \frac{A_{tube}}{\pi D_o L} \quad (22)$$

The final step is to calculate the effectiveness of the designed evaporator. This effectiveness is determined through testing. Use the following equation to determine the effectiveness of the evaporator [28]:

$$\varepsilon = \frac{q}{q_{max}}$$

If $C_h = C_{min}$,

$$\varepsilon = \frac{C_h (T_{h,in} - T_{h,out})}{C_{min} (T_{h,in} - T_{c,in})}$$

If $C_c = C_{min}$

$$\varepsilon = \frac{C_c (T_{h,in} - T_{h,out})}{C_{min} (T_{h,in} - T_{c,in})} \quad (23)$$

Data Collection Procedure

During the testing process, the ORC system continuously monitored multiple parameters, such as temperature, pressure, refrigerant flow rate, and generator output voltage. The temperature was accurately measured using a type K thermocouple with a precision of $\pm 0.5\%$ or $\pm 1^\circ\text{C}$ and connected to the Advantech data logger USB-4718. The pressure was manually recorded using a pressure gauge, which was installed at four designated test points on the system. These test points included Test Point 1 between the condenser outlets and the pump inlet, Test Point 2 between the pump outlets and the evaporator inlet, Test Point 3 between the exit of the evaporator and the entrance of the turbine, and Test Point 4 between the turbine exits and the pump inlet.

The refrigerant flow rate was measured directly by observing the flow meter. Each test lasted 30 minutes; temperature data on the ORC system was recorded automatically every minute, and pressure, temperature, and discharge data were recorded manually every 5 minutes.

RESULTS AND DISCUSSION

After completing the design calculations, a recapitulation of the overall results of the evaporator design calculations is obtained, which will be shown in [Table 1](#).

After the manufacture of the evaporator is complete, the evaporator assembly is carried out to the ORC system, where the evaporator will be connected to the exhaust of the gasoline engine, which will supply heat energy to the evaporator and the channel of the exhaust gas was shown in [Figure 3](#).

The ORC system front view and the rear view are shown in [Figure 4](#), at the front view shows ORC system components such as the condenser, turbine, temperature gauges and pressure gauges. While at the rear view shows an ORC system such as pump, a generator coupled to a turbine, and a flowmeter.

Table 1. Evaporator Design Result Data

Parameter	Evaporator Type Fin and Tube
Evaporator Length	0.46 m
Tube Length	41.4 m
Evaporator Fin Width	0.154 m
High Fin Evaporator	0.355 m
Total Area	14.324 m ²
Number of Tubes	90
Total Fin	135
Di and Do Tube	7.525 mm and 9.525 mm



Figure 3. Gasoline Engine Exhaust Heat and ORC System

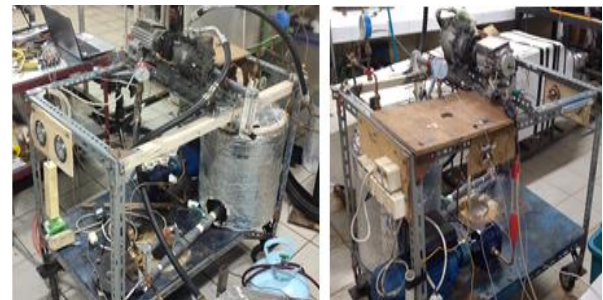


Figure 4. Front and Rear View ORC System

The evaporator that has been designed and has been assembled into ORC System is shown in [Figure 5](#). It is essential to conduct thorough testing to assess the efficiency of an ORC system utilizing a fin and tube type evaporator heat exchanger. This involves the installation of a thermocouple and pressure gauge at each input and output component within the ORC system. Additionally, a flow meter should be installed at the pump output to determine the fluid flow rate accurately.

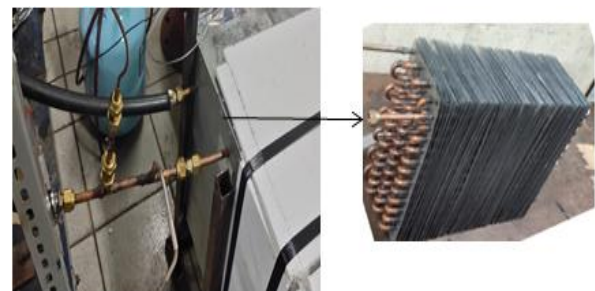


Figure 5. Evaporator on ORC system

Meanwhile, to enter and exit the exhaust gas/air on the evaporator, a thermocouple is installed, which serves to determine the temperature entering and leaving the evaporator. So that it can be seen how much energy is absorbed by the evaporator from the heat of the exhaust gas from the gasoline engine. Furthermore, if the test preparation has been completed, the gasoline engine is turned on until the exhaust heat entering the desired evaporator is reached, which is 95 °C.

After testing the ORC system using a fin-and-tube type evaporator, it is necessary to calculate the effectiveness of the evaporator to determine the performance of the designed evaporator using (23).

$$\varepsilon = \frac{C_h (T_{h,in} - T_{h,out})}{C_{min} (T_{h,in} - T_{c,in})}$$

$$\varepsilon = 95.38\%$$

Table 2 shows a summary of what the calculations showed about how well the evaporator worked at a temperature of 95 °C and a pressure of 12 bars.

In the ORC system testing that has been carried out when the incoming gas temperature is 95 °C and a pressure of 12 bar, the effectiveness of the designed evaporator is evident. Based on the test data, the exhaust gas temperature of the gasoline engine that enters the evaporator is 95 °C and the exit temperature is 44 °C, while the temperature of the refrigerant inlet is 41.53 °C and exits 54.2 °C, so that the effectiveness of the designed evaporator is 94.33%.

Figure 6 shows a comparison chart between effectiveness and pressure on the ORC system at a temperature of 95 °C.

Then the energy calculation in the ORC system is carried out. Testing and data collection in this study was carried out every 5 minutes for 30 minutes. From all the data obtained in the 25th minute, it shows that the efficiency of the ORC system is the highest efficiency result obtained after testing.

Table 2. Evaporator Effectiveness Temperature 95 °C and Pressure 12 Bar

Heat Capacity, Ch (kW/°C)	Cold Capacity, Cc (kW/°C)	Effectiveness (%)
0.029	0.0344	95.38
0.029	0.0489	94.70
0.029	0.0507	95.40
0.029	0.0507	94.34
0.029	0.0525	92.68
0.029	0.0543	93.48
Average Effectiveness		94.33

Table 3 summarizes the results of the calculations performed at 25 minutes on the test data. Table 3 shows the results of energy calculations in the ORC system with a fin-and-tube type evaporator as a heat exchanger that utilizes exhaust heat from a gasoline engine. In the ORC system, the efficiency of the system is 2.13%, with a mass flow rate of refrigerant of 0.0407 kg/s, turbine power generated at 0.4482 kJ/s, pump power at 0.2983 kJ/s, heat input at testing of when testing is 172.37 kJ/kg, and the net power produced by the ORC system at 0.15 kJ/s.

Some of the studies that have been done on the ORC generating system are listed in Table 4. Table 4 presents various studies using an ORC system with various types of heat sources. This research uses an ORC system with a heat source, namely the waste heat (exhaust heat) of a gasoline engine with the working fluid R134a. In this study, it is able to produce ORC theoretical power of 0.15 kW with an efficiency of 2.13%.

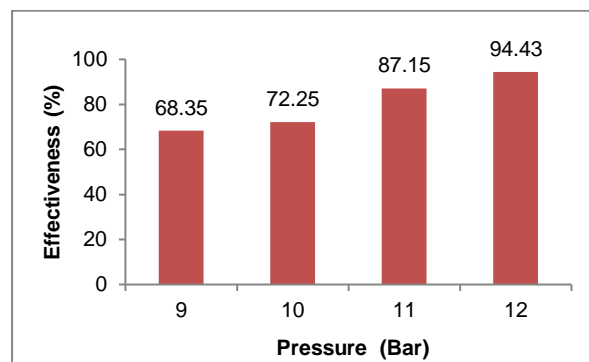


Figure 6. Comparison of Effectiveness to Pressure

Table 3. Energy Calculation of ORC system with Gasoline Engine Exhaust Heat

Variable	Value
Mass Flow Rate	0.0407 kg/s
Turbine Power	0.4482 kJ/s
Pump Power	0.2983 kJ/s
heat in	172.37 kJ/kg
W _{net}	0.15 kJ/s
System Efficiency	2.13 %

Table 4. Previous research on the ORC system

year	Researcher	Heat source, Working Fluid, Capacity, Efficiency
2019	Martin et al. [21]	Water Heater, R134a, 0.279 kW, 3.33 %
2019	Martin et al. [22]	Solar Collector, R134a, 0.305 kW, 4.29 %
2017	Ahmadi et al. [24]	Geothermal, R134a and R245fa, 1.7 kW and 22,5 kW respectively
2022	Currently research	Waste Heat, R134a, 0.15 kW, 2.13%

Table 4 provides a comprehensive overview of several studies conducted on ORC systems that utilize a range of heat sources, including water heaters, solar collectors, geothermal energy, and waste heat. One study focusing on waste heat, using R134a as the working fluid, reported that the ORC system could achieve an efficiency of up to 2%, despite the temperature difference between the heat source and the working fluid. The efficiency levels reported in the literature varied between 2-5%.

The current study investigates the potential of utilizing exhaust heat energy from a gasoline engine, which is an untapped resource. The findings demonstrate that an ORC system utilizing the exhaust heat of a gasoline engine can efficiently generate electricity. This approach presents a promising solution for utilizing waste heat and reducing reliance on non-renewable energy sources [28][29].

CONCLUSION

The research led to several conclusions. The fin and tube type evaporator designed for the study featured a total tube length of 41.4 m, 90 tubes, and 135 fins. During testing at a pressure of 12 bars and a 95 °C, the evaporator achieved an average effectiveness of 94.33%. The use of the fin-and-tube evaporator in an ORC system with exhaust heat from a gasoline engine resulted in the highest efficiency, reaching 2.13%. These findings demonstrate the potential of utilizing waste heat and indicate that the designed evaporator can be an effective solution for a wide range of ORC applications.

ACKNOWLEDGMENT

The author expresses gratitude to the Department of Mechanical Engineering at the University of Riau for providing technical support during the research.

REFERENCES

- [1] A. Martin, Miswandi, A. Prayitno, I. Kurniawan, and Romy, "Exergy analysis of gas turbine power plant 20 MW in Pekanbaru-Indonesia," *International Journal of Technology*, vol. 7, no. 5, pp. 921-927, 2016, doi: 10.14716/ijtech.v7i5.1329.
- [2] T. Bakirtas and A. G. Akpolat, "The relationship between energy consumption, urbanization, and economic growth in new emerging-market countries," *Energy*, vol. 147, pp. 110-121, 2018, doi: 10.1016/j.energy.2018.01.011.
- [3] Badan Pusat Statistika, "Statistik Indonesia 2020 Statistical Yearbook of Indonesia 2020," *Stat. Yearb. Indones.*, 2020.
- [4] BPPT, *Indonesia Energy Outlook 2020 - Special Edition Dampak Pandemi COVID-19 terhadap Sektor Energi di Indonesia Diterbitkan*. 2020.
- [5] A. Rokhmawati, "Comparison of power plant portfolios under the no energy mix target and national energy mix target using the mean-variance model," *Energy Reports*, vol. 7, pp. 4850-4861, 2021, doi: 10.1016/j.egyr.2021.07.137.
- [6] D. Kweku et al., "Greenhouse Effect: Greenhouse Gases and Their Impact on Global Warming," *Journal of Scientific Research and Reports*, vol. 17, no. 6, pp. 1-9, 2018, doi: 10.9734/jsrr/2017/39630.
- [7] O. Aboelwafa, S. E. K. Fateen, A. Soliman, and I. M. Ismail, "A review on solar Rankine cycles: Working fluids, applications, and cycle modifications," *Renewable and Sustainable Energy Reviews*, vol. 82, no. 1, pp. 868-885, 2018, doi: 10.1016/j.rser.2017.09.097.
- [8] W. M. Waseq, "The impact of air pollution on human health and Environment with mitigation Measures to reduce Air Pollution in Kabul Afghanistan," *International Journal of Healthcare Sciences*, vol. 8, no. 1, pp. 1-12, 2020.
- [9] A. Rahman, O. Farrok, and M. M. Haque, "Environmental impact of renewable energy source based electrical power plants: Solar, wind, hydroelectric, biomass, geothermal, tidal, ocean, and osmotic," *Renewable and Sustainable Energy Reviews*, vol. 161, p. 112279, Jun. 2022, doi: 10.1016/J.RSER.2022.112279.
- [10] I. E. Agency, *Energy Technology Perspectives 2017 - Catalysing Energy Technology Transformations*. France:IEA Publications,2017.doi: 10.1787/energy_tech-2017-en.
- [11] Q. Sun, Y. Wang, Z. Cheng, J. Wang, P. Zhao, and Y. Dai, "Thermodynamic and economic optimization of a double-pressure organic Rankine cycle driven by low-temperature heat source," *Renewable Energy*, vol. 147, pp. 2822-2832, 2020, doi: 10.1016/j.renene.2018.11.093.
- [12] F. Wang, L. Wang, H. Zhang, L. Xia, H. Miao, and J. Yuan, "Design and optimization of hydrogen production by solid oxide electrolyzer with marine engine waste heat recovery and ORC cycle," *Energy Conversion and Management*, vol. 229, p. 113775, 2021, doi: 10.1016/j.enconman.2020.113775.
- [13] A. Martin, R. Romy, D. Agustina, and A. M. Ibra, "Design and manufacturing of organic

- rankine cycle (orc) system using working fluid r-134a with helical evaporator and condenser," *IOP Conference Series: Materials Science and Engineering*, vol. 539, no. 1, 2019, doi: 10.1088/1757-899X/539/1/012027.
- [14] H. Tian, P. Liu, and G. Shu, "Challenges and opportunities of Rankine cycle for waste heat recovery from internal combustion engine," *Progress in Energy and Combustion Science*, vol. 84, pp. 100906, 2021, doi: 10.1016/j.pecs.2021.100906
- [15] Z. G. Shen, L. L. Tian, and X. Liu, "Automotive exhaust thermoelectric generators: Current status, challenges and future prospects," *Energy Conversion and Management*, vol. 195, pp. 1138-1173, 2019, doi: 10.1016/j.enconman.2019.05.087.
- [16] M. A. Chatzopoulou, S. Lecompte, M. De Paepe, and C. N. Markides, "Off-design optimisation of organic Rankine cycle (ORC) engines with different heat exchangers and volumetric expanders in waste heat recovery applications," *Applied Energy*, vol. 253, 2019, doi: 10.1016/j.apenergy.2019.113442.
- [17] S. P. Dutta and R. Chandra Borah, "Design of a Solar Organic Rankine Cycle Prototype for 1 kW Power Output," *International Journal of Engineering Trends and Technology*, vol. 62, no. 1, 2018, doi: 10.14445/22315381/ijett-v62p205.
- [18] R. Pili, L. García Martínez, C. Wieland, and H. Spliethoff, "Techno-economic potential of waste heat recovery from German energy-intensive industry with Organic Rankine Cycle technology," *Renewable and Sustainable Energy Reviews*, vol. 134, no. September, p. 110324, 2020, doi: 10.1016/j.rser.2020.110324.
- [19] W. Zhang, F. Yang, H. Zhang, X. Ping, and D. Yan, "Numerical analysis and optimization design of fin-and-tube evaporator in organic Rankine cycle system for diesel engine waste heat recovery," *International Journal of Heat and Mass Transfer*, vol. 175, p. 121376, 2021, doi: 10.1016/j.ijheatmasstransfer.2021.121376.
- [20] A. Anastasovski, P. Rasković, and Z. Guzović, "A review of heat integration approaches for organic rankine cycle with waste heat in production processes," *Energy Conversion and Management*, vol. 221, 2020, doi: 10.1016/j.enconman.2020.113175.
- [21] A. Martin, C. Naibaho, I. Kurniawan, and Romy, "Design and Manufacturing of Organic Rankine Cycle (ORC) System Using R-134a as Working Fluid with Solar Collector as Source Energy," *IOP Conference Series: Materials Science and Engineering*, 2019, doi: 10.2991/iccelst-st-19.2019.8.
- [22] A. Martin, R. Romy, D. Agustina, and A. M. Ibra, "Experimental study of an organic rankine cycle system using r134a as working fluid with helical evaporator and condenser," *IOP Conference Series: Materials Science and Engineering*, 2019, doi:10.1088/1757-899X/539/1/012026.
- [23] R. Loni et al., "A review of solar-driven organic Rankine cycles: Recent challenges and future outlook," *Renewable and Sustainable Energy Reviews*, vol. 150, no. June, p. 111410, 2021, doi: 10.1016/j.rser.2021.111410.
- [24] A. Ahmadi et al., "Applications of geothermal organic Rankine Cycle for electricity production," *Journal of Cleaner Production*, vol. 274, 2020, doi: 10.1016/j.jclepro.2020.122950.
- [25] S. Sudiono, R. Sundari, and R. Anggraini, "Fiberglass Circular Turbulator in Counter Flow Double Pipe Heat Exchanger: a Study of Heat Transfer Rate and Pressure Drop," *SINERGI*, vol. 25, no. 1, pp. 51-58, 2020, doi: 10.22441/sinergi.2021.1.007.
- [26] D. Romahadi, N. Ruhyat, and L. B. Desti Dorion, "Condensor Design Analysis With Kays and London Surface Dimensions," *SINERGI*, vol. 24, no. 2, pp. 81-86, 2020, doi: 10.22441/sinergi.2020.2.001.
- [27] W. M. Kays and A. L. London, *Compact heat exchangers*, Third Edition, New York: McGraw-Hill, 2018.
- [28] J. H. Lienhard IV and J. H. Lienhard V, *A Heat Transfer Textbook*, Fifth Edition, Massachusetts: Phlogiston Press, 2020.
- [29] N. Ruhyat et al., "Hydrodynamic study of drying on Qisthi Hindi using a Fluidized Bed Dryer," *Journal of Integrated and Advanced Engineering (JIAE)*, vol. 2, no. 2, pp. 97-106, 2022, doi: 10.51662/jiae.v2i2.67